Accelerated Publication

THE JOURNAL OF BIOLOGICAL CHEMISTRY
Vol. 279, No. 25, Issue of June 18, pp. 25939–25942, 2004

Crystal Structure of the Membrane Fusion Protein, MexA, of the Multidrug Transporter in *Pseudomonas aeruginosa**[S]

Received for publication, April 13, 2004,
and in revised form, April 26, 2004
Published, JBC Papers in Press, April 26, 2004,
DOI 10.1074/jbc.C400164200

Hiroyuki Akama‡, Takanori Matsuura§, Sachiko Kashiwagi‡, Hiroshi Yoneyama‡¶, Shin-ichiro Narita‡, Tomitake Tsukihara§, Atsushi Nakagawa§‖, and Taiji Nakae‡**

From the ‡Department of Molecular Life Science, Tokai University School of Medicine, Isehara, 259-1193, Japan and the §Institute for Protein Research, Osaka University, Suita 565-0871, Japan

The MexAB-OprM efflux pump of *Pseudomonas aeruginosa* is central to multidrug resistance of this organism, which infects immunocompromised hospital patients. The MexA, MexB, and OprM subunits were assumed to function as the membrane fusion protein, the body of the transporter, and the outer membrane channel protein, respectively. For better understanding of this important xenobiotic transporter, we show the x-ray crystallographic structure of MexA at a resolution of 2.40 Å. The global MexA structure showed unforeseen new features with a spiral assembly of six and seven protomers that were joined together at one end by a pseudo 2-fold image. The protomer showed a new protein structure with a tandem arrangement consisting of at least three domains and presumably one more. The rod domain had a long hairpin of twisted coiled-coil that extended to one end. The second domain adjacent to the rod α-helical domain was globular and constructed by a cluster of eight short β-sheets. The third domain located distal to the α-helical rod was globular and composed of seven short β-sheets and one short α-helix. The 13-mer was shaped like a woven rattan cylinder with a large internal tubular space and widely opened flared ends. The 6-mer and 7-mer had a funnel-like structure consisting of a tubular rod at one side and a widely opened flared funnel top at the other side. Based on these results, we constructed a model of the MexAB-OprM pump assembly. The three pairs of MexA dimers interacted with the periplasmic α-barrel domain of OprM via the α-helical hairpin, the second domain interacted with both MexB and OprM at their contact site, and the third and disordered domains probably interacted with the distal domain of MexB. In this fashion, the MexA subunit connected MexB and OprM, indicating that MexA is the membrane bridge protein.

Emergence of infectious agents resistant to structurally and functionally dissimilar chemotherapeutic agents is increasingly problematic in human health. An important factor contributing to this multidrug resistance is the drug or xenobiotic efflux pump, which lowers the intracellular drug concentration by exporting incoming chemotherapeutic agent across the membranes. *Pseudomonas aeruginosa* easily infects immunocompromised hospital patients, and this low virulent bacterium often is life-threatening. A problem associated with *P. aeruginosa* infection is that this organism shows a broad spectrum of intrinsic and mutational resistances to structurally and functionally dissimilar antibiotics (1–6). These multiantibiotic resistances in this organism are largely attributable to the expression of multidrug efflux pumps (7, 8). The *P. aeruginosa* chromosome encodes several drug exporter genes, and among them, MexAB-OprM is central to both intrinsic and mutational multidrug resistance.

The resistance nodulation division (RND)[1] family efflux pump, including MexAB-OprM, consists of three membrane bound subunits, such as MexA, MexB, and OprM, anchoring the inner and outer membranes, respectively (4, 5, 9–11). The MexB subunit is central to the pump function, which spans the cytoplasmic membrane 12 times, selects antibiotics to be exported, and is assumed to transport the substrates expending the energy of the proton gradient across the cytoplasmic membrane (12–14). The crystal structure of an MexB homologue, AcrB of *Escherichia coli*, showed that the protein consisted mainly of three domains: the membrane spanning domain, the pore domain, and the TolC docking domain (15).

The OprM subunit is the outer membrane-anchored lipoprotein that is assumed to play a role in the final step of antibiotic extrusion facilitating the exit of antibiotic across the outer membrane (5, 16, 17). Structural analysis of the OprM homologue, TolC of *E. coli*, revealed that the trimeric assemblies of the protomer consisted largely of two domains: an outer membrane spanning the β-barrel and a long α-helical barrel extended to the periplasmic space (18).

The MexA subunit anchors an inner membrane via fatty acid(s) attached to the N-terminal cysteine residue (5, 16, 19, 20). Presence of the membrane fusion protein is indispensable

* This work was supported in part by a grant-in-aid for the 21st Century Centers of Excellence Research and the National Project on Protein Structural and Functional Analyses from the Ministry of Education, Culture, Sport, Science and Technology; a grant-in-aid from the New Energy and Industrial Technology Department Organization (NEDO); a Tokai University Project Research Grant; and by a Tokai University School of Medicine Research Project Grant. The costs of publication of this article were defrayed in part by the payment of page charges. This article must therefore be hereby marked "*advertisement*" in accordance with 18 U.S.C. Section 1734 solely to indicate this fact.

[S] The on-line version of this article (available at http://www.jbc.org) contains Table I and supplemental material for "Results and Discussion."

The atomic coordinates and structure factors (code 1VF7) have been deposited in the Protein Data Bank, Research Collaboratory for Structural Bioinformatics, Rutgers University, New Brunswick, NJ (http://www.rcsb.org/).

¶ Present address: Faculty of Agriculture, Tohoku University, Sendai 981-8555, Japan.

‖ To whom correspondence may be addressed: The Inst. for Protein Research, Osaka University, Suita 565-0871, Japan. Tel./Fax: 81-6-6879-4313; E-mail: atsushi@protein.osaka-u.ac.jp.

** To whom correspondence may be addressed: Dept. of Molecular Life Science, Tokai University School of Medicine, Isehara, 259-1193, Japan. Tel.: 81-463-93-5436; Fax: 81-463-93-5437; E-mail: nakae@is.icc.u-tokai.ac.jp.

[1] The abbreviations used are: RND, resistance nodulation cell division; MFP, membrane fusion protein; SIRAS, single isomorphous replacement with anomalous scattering.

in xenobiotic export by the RND family proteins (1, 21, 22). Deletion of the fatty acyl moiety liberates the protein from the membrane, and the protein became freely soluble in aqueous solutions. This mutant protein had a fully functional antibiotic efflux (19) and, therefore, it was assumed that the entire protein moiety of MexA protruded to the periplasmic aqueous space. The MexA subunit and its homologue proteins were, therefore, assumed to connect the inner and outer membrane subunits and hence designated as the membrane fusion protein (MFP) (16). However, the precise structure and function of the MFPs remain to be clarified. For better understanding of the MFPs, we analyzed the x-ray crystal structure of MexA of *P. aeruginosa*, and here we report its structure.

EXPERIMENTAL PROCEDURES

Bacterial Cell, Culture Conditions, and Cell Fractionation—The bacterial strain used was *P. aeruginosa* TNP070 lacking chromosomal *mexA* (21). The pAzu-MexA plasmid was a derivative of pMMB67EH/HE carrying the Azu-MexA-$(His)_6$ fusion gene as described previously (19). TNP070 was transformed with pAzu-MexA, and this was used throughout this study. Cells were grown in L-broth at 37 °C with shaking at 220 rpm to $A_{600}^{1.0\ cm}$ = 0.7. Isopropyl-1-thio-β-D-galactoside was added to the concentration of 0.5 mM and shaken as above for an additional 2.5 h. The cells were harvested by centrifugation at 24 °C, suspended in a buffer containing 50 mM Tris-HCl, pH 7.2, 0.2 mM $MgCl_2$, and a tablet of the protease inhibitor mixture (Roche Applied Science, Complete Mix) and subjected to cold-shock treatment by alternatively immersing the cell suspension in water baths at 37 and 0 °C three times (17). The cell suspension was centrifuged at 10,000 × *g* for 10 min at 4 °C, and the supernatant fraction was centrifuged again at 150,000 × *g* for 60 min at 4 °C. The soluble fraction was retained for further treatment.

Purification of the MexA-$(His)_6$—The cold-shock material from 1 liter of culture was mixed with a 2-ml packed volume of nickel-nitrilotriacetic acid-Sepharose resin (Invitrogen, ProBond) and gently stirred at 4 °C for 15 min. The resin suspension was packed into an open column, washed with 20 ml of the washing buffer containing 50 mM sodium phosphate, pH 7.2, 0.3 M NaCl, and 20 mM imidazole. Next, the column was eluted with a buffer containing 50 mM sodium phosphate, pH 7.2, 0.3 M NaCl, 250 mM imidazole. The yield of homogeneously purified MexA was consistently 6–7 mg/liter of culture. Purified MexA was subjected to dialysis against a large excess of 20 mM HEPES, pH 7.2, 0.3 M LiCl, 80 mM imidazole overnight with several changes of dialysis buffer. The protein concentration was adjusted to 10 mg/ml using the Vivaspin concentrator (VivaScience).

Crystallization—The hanging-top vapor diffusion technique was used throughout this study. Five parts of MexA (10 mg/ml) in the dialysis buffer was mixed with 4 parts of the reservoir buffer containing 60 mM HEPES, pH 7.2, 40 mM Tris-HCl, pH 7.2, 10% of glycerol, 3% of 2-methyl-2,4-pentandiol, and 26–28% polyethylene glycol 1000 and one part of the additive (50% Jeffamine-M600, pH 7.0, Hampton Research). The setup mixture was kept at 20 °C in an incubator for 1–2 weeks. The rod-shaped MexA crystals grew to the size of about 0.7 × 0.5 × 0.3 mm^3. The space group was $P2_1$ with cell dimensions of a = 130.0 Å, b = 180.3 Å, c = 214.2 Å, β = 107.0°.

Diffraction Data Collection—Diffraction data for structure determination were collected at beamlines of the synchrotron facilities of Photon Factory (Ibaraki, Japan) and SPring-8 (Hyogo, Japan). Diffraction data of native MexA were collected on the DIP6040 imaging plate/CCD hybrid detector (MacScience, Bruker-AXS) at BL44XU at SPring-8 (Native 1) and on the Quantum 4R CCD detector (Area Detector System Corp.) at BL6A at the Photon Factory (Native 2). Diffraction data of the Lu derivative, which was prepared by soaking in 2 mM $Lu(O_2C_2H_5)_2$ for 2 h, were collected on the Quantum 210 CCD detector (Area Detector System Corp.) at AR-NW12 at the Photon Factory. The diffraction images were reduced, scaled, and merged with the HKL2000 package (23). The intensities were then converted to the structure factor amplitudes with TRUNCATE in CCP4 (24). Summary of crystallographic data and refinement statistics are given in Table I in the supplemental material.

Structure Determination—The single isomorphous replacement with the anomalous scattering (SIRAS) method using the Lu derivative was applied to solve the crystallographic phase problem. Native 2 data were used as a native data set for phase determination. Initially six Lu sites were located using SHELX-97 (25). Heavy atom parameter refinement and SIRAS phasing were carried out using the program SHARP (26).

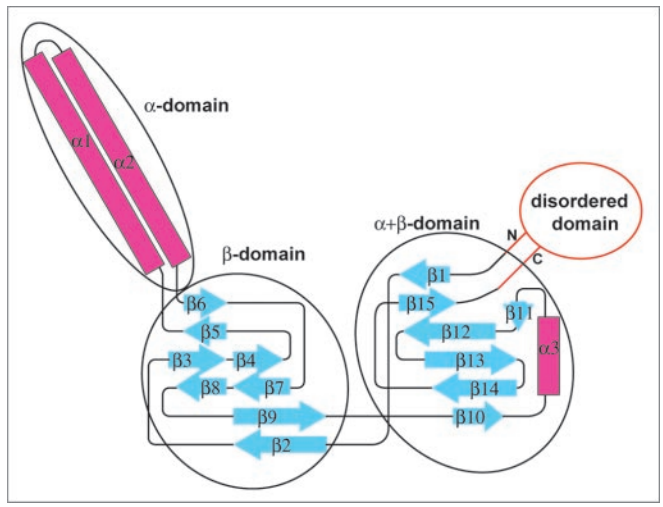

FIG. 1. **Two-dimensional topology models of MexA.** The two-dimensional model was constructed on the basis of the x-ray crystallographic data and the DSSP program (42). Localization of α-helices and β-sheets was arbitrary and that of each domain was simplified to ease understanding of the relative position. *Columns* and *arrows* indicate α-helices (*magenta*) and β-sheets (*cyan*).

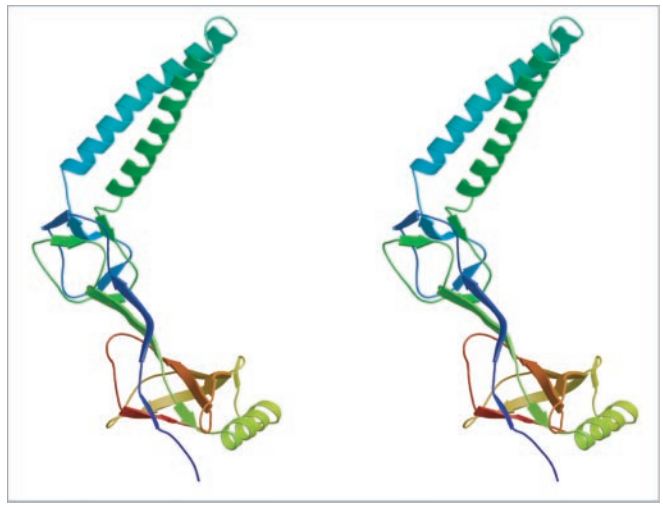

FIG. 2. **Stereo view of the MexA monomer.** Ribbon model of the MexA monomer: gradient rainbow color of *blue* to *red* indicates N- to C-terminal.

Minor sites of heavy atoms were found subsequently in residual maps after the refinement of heavy atom parameters by SHARP, and finally 14 Lu sites were included for phase calculation. Phase improvement using the density modification technique with SOLOMON (27) and DM (28) integrated in SHARP was applied. The atomic model was built using program O (29) and refined against the native 1 data set. At the initial stage of refinement, a simulated-annealed torsion angle refinement using CNS (30) was applied. Subsequent cycles of manual revision of the atomic model using program O and restrained-parameter maximum-likelihood refinement carried out by REFMAC5 (31) in CCP4 (24) were conducted to refine the atomic structure.

RESULTS AND DISCUSSION

Structural Analysis—The SIRAS method using the $Lu(O_2C_2H_5)_2$ was applied using SHARP (26). The atomic model was built using program O (29) and then refined using CNS (30) and refmac5 (31). Details of structure analysis were given in the section of supplemental materials.

Overall Structure of the Monomer—At the current stage of refinement, 68.3% of the residues were visible. N- and C-terminal residues provided little structural information. The best ordered monomer structure shows 252 residues (from 23 to 274) among 369 amino acid residues of Azu-MexA-$(His)_6$. The

overall structure showed that the MexA monomer consisted mainly of three domains and possibly one additional unseen domain due to a disorder as follows (Figs. 1 and 2). (i) At one end, two α-helices (from Ala^{74} to Ala^{102} and from Lys^{108} to Arg^{133}) formed a long left-hand twisted α-helical hairpin structure designated as the α-domain. (ii) The globular domain adjacent to the α-helical domain consisted of eight short β-sheets designated as the β-domain. This domain shows a topology similar to the biotinyl/lipoyl carrier proteins and domains family was defined in the SCOP data base (32). (iii) Another globular domain adjacent to the central β-domain, distal to the α-domain, was composed of seven short β-strands and one short α-helix designated as the $\alpha+\beta$-domain. (iv) The poorly solved disordered domain contained the N- and C-terminal regions (Fig. 1). There was a turn of about +60° against the α-helix hairpin at the loops between the α-domain and the β-domain forming a sickle shape (Fig. 2). The topological arrangement of α- and β-domains agreed well with the predicted model (33).

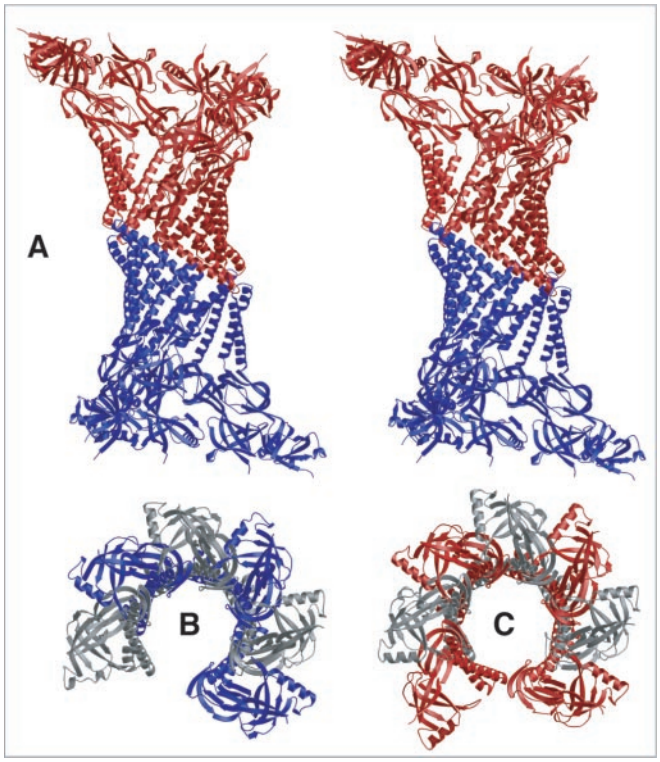

FIG. 3. **Ribbon diagrams of a representative MexA structure.** *A*, stereo side view of the structure of the tridecamer. Heptamer and hexamer are colored *red* and *blue*, respectively. *B*, bottom view of Fig. 1*A* (hexamer). Each monomer is distinguished by alternatively changing the color to *blue* and *gray*, respectively. *C*, top view of Fig. 1*A* (heptamer). Each monomer is distinguished by alternatively changing the color to *red* and *gray*, respectively. The figures were drawn by MolScript version 2.1.2 (40) and Raster 3D version 2.7b (41).

Overall Structure of the Tridecamer (13-mer)—The crystal structure of MexA appeared as a spiral assembly of the 13 protomer by contiguous joining of the hexamer and heptamer forming a rod at the middle and a funnel-top structure at both ends (Fig. 3*A*). The 13-mer had an internal space with widely opened ends. The hexamer and heptamer were spirally assembled with a side-by-side contiguity of each monomer so that the spiral structure continued until the first molecule touched the seventh molecule at the narrower end, but the wider part of the first and last molecules remained untouched exhibiting a large unsealed lateral side (Fig. 3, *B* and *C*). At the end of the heptamer, the orientation of the protomer was inverted, and the spiral assembly of the hexamer continued along one end of the heptamer. The structure of the hexamer and heptamer may be divided into two parts; one domain is a tightly packed barrel structure with anti-parallel arranged α-helices and another is a widely opened petal-like structure mainly formed by two (or more) globular domains mostly composed of the β-barrel structure.

Assembly Model of the MexAB-OprM Efflux Pump—As we constructed the MexA model, it was of great interest to fit this newly obtained MexA structure to that of the MexB and OprM subunits and envisages the structure of the whole transporter assembly. One may ask whether or not MexA, MexB, and OprM interact each other. We examined interaction of MexB and OprM with tagged MexA and found by the immunoblotting method that non-tagged MexB and OprM were copurified with tagged MexA suggesting that these three subunits are in complex *in vivo*.[2] Since the three-dimensional structures of MexB and OprM is not yet available, they were simulated by amino acid replacement of the MexB and OprM instead of their homologues, AcrB and TolC of *E. coli*, respectively, and molecular models were constructed.

At first, it was necessary to determine the orientation of the MexA structure. Since MexA was mainly located in the inner membrane fraction (19), and the N-terminal end of MexA was fatty acid-modified, it is highly likely that at least one end of MexA anchored the inner membrane (19). Since the N- and

[2] E. Mokhonova, V. Mokhonov, and T. Nakae, manuscript in preparation.

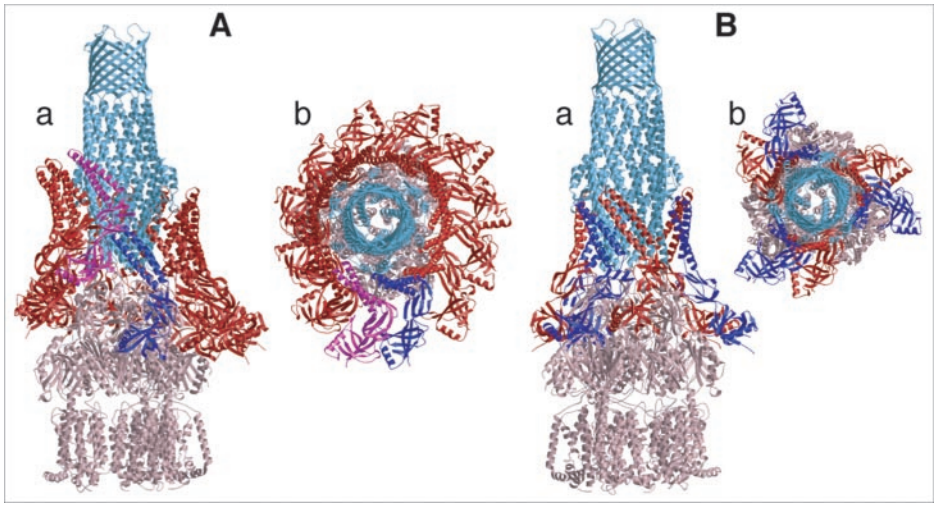

FIG. 4. **Fitting model of the MexA structure to MexB and OprM.** MexA, MexB, and OprM are colored *red*, *pink*, and *light sky-blue*, respectively. *A*, the figure is drawn on the basis of the sleeve model. The first and twelfth molecules are distinguished by *magenta* and *blue* colors, respectively. Symbols: *a*, a side view; *b*, a vertical view from the OprM side. *B*, figure is based on the 3-fold MexA-dimer model. Two MexA molecules in the dimer are distinguished by *blue* and *red* colors, respectively. Symbols: *a*, a side view; *b*, a vertical view from the OprM side.

C-terminal ends of MexA were located at the disordered domain adjacent to the $\alpha+\beta$-domain, MexA must be oriented with the $\alpha+\beta$-domain located proximal to MexB and the α-domain directed toward OprM. Lines of evidence support this conclusion. (i) The domain swapping experiments between AcrA of *E. coli* and its homologue protein suggested that the C-terminal proximal region of AcrA is important in the interaction with AcrB (34). (ii) AcrA was chemically cross-linked with AcrB (35).

The first question to be answered was whether or not the MexA 13-mer is present in intact cells. Although an approximate longitudinal size of the 13-mer agreed well with the distance between the inner and outer membranes (36), we assume that the 13-mer is most likely a crystallographic artifact by the reasons that MexA is mainly fractionated with the inner membrane and the $\alpha+\beta$-domain is located at both ends of the 13-mer (Fig. 3*A*). The next question was whether or not the spiral assembly of MexAs exists in the cells. The first model we present is the sleeve model based on the structure of MexA in which an MexA sleeve holds the distal domains of MexB, and the α-helical domains of MexA interact with OprM (Fig. 4*A*). This simple model fitted well with the predicted function of MexA; however, the interior space of the sleeve appeared to be too small to accommodate the MexB and OprM junction, and also the spiral structure of MexA was less compatible with the flat configuration of MexB and OprM. Yet, it is conceivable that MexA winds around the MexB-OprM interaction site laterally (Fig. 4*A*). We calculated that a total 12 of MexA molecules might be needed to wind around a MexB-OprM trimer. Thus, we have not yet discarded this model.

The second model we would like to offer is the 3-fold MexA-dimer model that interacts with an MexA-OprM trimer (Fig. 4*B*). This subunit stoichiometry is based on our quantitative determination in intact cells of the individual subunit that five to six molecules of MexA are present per trimer of MexB and OprM (37). Presence of the dimeric MexA was supported by gel filtration experiments in which a small fraction of MexA was eluted in the position corresponding to the dimer, although the majority of MexA appeared to be monomeric in aqueous solution (data not shown). Fitting of α-helices of the MexA dimer with the lower part of OprM resulted in good helix-helix interaction of OprM and MexA with a contact angle of about 20° (Fig. 4*B*). This 20°-angle contact of the α-helices was supported by a report that the second most abundant α-helix contact was a 20° angle (38). Thus, it is likely that MexA and OprM interact by means of the respective α-helices. Consequently, the globular β-domain in the middle of the MexA fits with the MexB-OprM contact region, where a gap was formed. The globular $\alpha+\beta$-domains and disordered domain may have interacted with the MexB trimer. The disordered region is likely to have interacted with MexB as suggested with AcrA of *E. coli* (34).

Three models have been proposed for a possible mechanical role of MFP based on the sequence alignment study (33); a fully extended MFP directly bridges the inner and outer membranes; the α-helical hairpins is located parallel to the membrane domain; a α-helical hairpin interacts with the outer membrane subunits, and the remaining domains anchor to the inner membrane. Our crystal structure of MexA supports none of these proposals. The two-dimensional crystals of AcrA were subjected to electron cryography (39). The 20-Å resolution model predicted the presence of a central opening with a diameter of about 30 Å, which is in fairly good agreement with the present result. However, the global structure based on the two-dimensional crystals was largely different from that elucidated from x-ray crystallography.

Acknowledgments—We are grateful to the beamline staffs of SPring8 BL44XU (E. Yamashita and M. Yoshimura) and Photon Factory BL6A, AR-NW12 (N. Igarashi, N. Matugaki, and M. Suzuki) for their assistance in data collection. T. N. thanks Jurg P. Rosenbusch and Tilman Schirmer of Biozentrum, University of Basel, for their initial instruction on membrane protein crystallization.

REFERENCES

1. Li, X. Z., Nikaido, H., and Poole, K. (1995) *Antimicrob. Agents Chemother.* **39,** 1948–1953
2. Morshed, S. R., Lei, Y., Yoneyama, H., and Nakae, T. (1995) *Biochem. Biophys. Res. Commun.* **210,** 356–362
3. Poole, K., Heinrichs, D. E., and Neshat, S. (1993) *Mol. Microbiol.* **10,** 529–544
4. Poole, K. (2001) *J. Mol. Microbiol. Biotechnol.* **3,** 255–263
5. Paulsen, I. T., Park, J. H., Choi, P. S., and Saier, M. H., Jr. (1997) *FEMS Microbiol. Lett.* **156,** 1–8
6. Rella, M., and Haas, D. (1982) *Antimicrob. Agents Chemother.* **22,** 242–249
7. Saito, K., Eda, S., Maseda, H., and Nakae, T. (2001) *FEMS Microbiol. Lett.* **195,** 23–28
8. Srikumar, R., Paul, C. J., and Poole, K. (2000) *J. Bacteriol.* **182,** 1410–1414
9. Dong, Q., and Mergeay, M. (1994) *Mol. Microbiol.* **14,** 185–187
10. Paulsen, I. T., Brown, M. H., and Skurray, R. A. (1996) *Microbiol. Rev.* **60,** 575–608
11. Tseng, T. T., Gratwick, K. S., Kollman, J., Park, D., Nies, D. H., Goffeau, A., and Saier, M. H. (1999) *J. Mol. Microbiol. Biotechnol.* **1,** 107–125
12. Guan, L., Ehrmann, M., Yoneyama, H., and Nakae, T. (1999) *J. Biol. Chem.* **274,** 10517–10522
13. Eda, S., Maseda, H., and Nakae, T. (2003) *J. Biol. Chem.* **278,** 2085–2088
14. Guan, L., and Nakae, T. (2001) *J. Bacteriol.* **185,** 1734–1739
15. Murakami, S., Nakashima, R., and Yamaguchi, A. (2002) *Nature* **419,** 587–593
16. Ma, D., Cook, D. N., Hearst, J. E., and Nikaido, H. (1994) *Trends Microbiol.* **2,** 489–493
17. Nakajima, A., Sugimoto, Y., Yoneyama, H., and Nakae, T. (2000) *J. Biol. Chem.* **275,** 30064–30068
18. Koronakis, V., Sharff, A., Koronakis, E., Luisi, B., and Hughes, C. (2000) *Nature* **405,** 914–919
19. Yoneyama, H., Maseda, H., Kamiguchi, H., and Nakae, T. (2000) *J. Biol. Chem.* **275,** 4628–4634
20. Dinh, T., Paulsen, I. T., and Saier, M. H., Jr. (1994) *J. Bacteriol.* **176,** 3825–3831
21. Yoneyama, H., Ocaktan, A., Tsuda, M., and Nakae, T. (1997) *Biochem. Biophy. Res. Commun.* **233,** 611–618
22. Poole, K., Krebes, K., McNally, C., and Neshat, S. (1993) *J. Bacteriol.* **175,** 7363–7372
23. Otwinowski, Z., and Minor, W. (1997) *Methods Enzymol.* **276,** 307–326
24. Collaborative Computational Project No. 4 (CCP4) (1994) *Acta Crystallogr. Sect. D Biol. Crystallogr.* **50,** 760–763
25. Sheldrick, G. (1997) *Methods Enzymol.* **276,** 628–641
26. de la Fortelle, E., and Bricogne, G. (1997) *Methods Enzymol.* **276,** 472–494
27. Abrahams, J. P., and Leslie, A. G. W. (1996) *Acta Crystallogr. Sect. D Biol. Crystallogr.* **52,** 30–42
28. Cowtan, K. (1994) *Joint CCP4 and EST-EACBM Newslett. Protein Crystallogr.* **31,** 34–38
29. Jones, T. A., Zou, J. Y., Cowan, S. W., and Kjeldgaard, M. (1991) *Acra Crystallogr. Sect. A* **47,** 110–119
30. Brunger, A. T., Adams, P. D., Clore, G. M., DeLano, W. L., Gros, P., Grosse-Kunstleve, R. W., Jiang, J. S., Kuszewski, J., Nilges, M., Pannu, N. S., Read, R. J., Rice, L. M., Simonson, T., and Warren, G. L. (1998) *Acta Crystallgor. Sect. D Biol. Crystallogr.* **54,** 240–255
31. Murshudov, G. N., Vagin, A. A., and Dodson, E. J. (1997) *Acta Crystallogr. Sect. D Biol. Crystallogr.* **53,** 240–255
32. Murzin, A. G., Brenner, S. E., Hubard, T., and Chothia, C. (1995) *J. Mol. Biol.* **247,** 536–540
33. Johnson, J. M., and Church, G. M. (1999) *J. Mol. Biol.* **287,** 695–715C. G.
34. Elkins, C. A., and Nikaido, H. (2003) *J. Bacteriol.* **185,** 5349–5356
35. Zgurskaya, H. I., and Nikaido, H. (2000) *J. Bacteriol.* **182,** 4264–4267
36. Graham, L. L., Beveridge, T. J., and Nanninga, N. (1991) *Trends Biochem. Sci.* **16,** 328–329
37. Narita, S.-I., Eda, S., Yoshihara, E., and Nakae, T. (2003) *Biochem. Biophys. Res. Commun.* **308,** 922–926
38. Branden, C., and Tooze, J. (1991) *Introduction to Protein Structure*, 2nd Ed., p. 41, Garland Publishers, New York
39. Avila-Sakar, A. J., Misaghi, S., Wilson-Kubalek, E. M., Downing, K. H., Zgurskaya, H., Nikaido, H., and Nogales, E. (2001) *J. Struct. Biol.* **136,** 81–88
40. Kraulis, P. J. (1991) *J. Appl. Crystallogr.* **24,** 946–950
41. Merritt, E. A., and Bacon, D. V. (1997) *Methods Enzymol.* **277,** 505–524
42. Kabsch, W., and Sander, C. (1983) *Biopolymers* **22,** 2577–2637

Crystal Structure of the Membrane Fusion Protein, MexA, of the Multidrug Transporter in *Pseudomonas aeruginosa*

Hiroyuki Akama, Takanori Matsuura, Sachiko Kashiwagi, Hiroshi Yoneyama, Shin-ichiro Narita, Tomitake Tsukihara, Atsushi Nakagawa and Taiji Nakae

J. Biol. Chem. 2004, 279:25939-25942.
doi: 10.1074/jbc.C400164200 originally published online April 26, 2004
